Published in final edited form as:
Cell Metab. 2012 April 4; 15(4): 534–544. doi:10.1016/j.cmet.2012.02.011.

Autophagy Links Inflammasomes to Atherosclerotic Progression

Babak Razani[1,2], **Chu Feng**[1], **Trey Coleman**[1], **Roy Emanuel**[1], **Haitao Wen**[5], **Seungmin Hwang**[4], **Jenny P. Ting**[5], **Herbert W. Virgin**[4], **Michael B. Kastan**[6], and **Clay F. Semenkovich**[1,3]

[1]Department of Medicine, Division of Endocrinology, Metabolism & Lipid Research, Washington University School of Medicine, St. Louis MO 63110

[2]Cardiovascular Division, Washington University School of Medicine, St. Louis MO 63110

[3]Department of Cell Biology & Physiology, Washington University School of Medicine, St. Louis MO 63110

[4]Department of Pathology & Immunology, Washington University School of Medicine, St. Louis MO 63110

[5]Department of Microbiology & Immunology, University of North Carolina, Chapel Hill, NC 27599

[6]Department of Oncology, St. Jude Children's Research Hospital, Memphis, TN 38105

SUMMARY

We investigated the role of autophagy in atherosclerosis. During plaque formation in mice, autophagic markers co-localized predominantly with macrophages (mϕ). Atherosclerotic aortas had elevated levels of p62, suggesting that dysfunctional autophagy is characteristic of plaques. To determine if autophagy directly influences atherogenesis, we characterized Beclin-1 heterozygous-null and mϕ-specific ATG5-null (ATG5-mϕKO) mice, commonly used models of autophagy haploinsufficiency and deficiency, respectively. Haploinsufficent Beclin-1 mice had no atherosclerotic phenotype, but ATG5-mϕKO mice had increased plaques suggesting an essential role for basal levels of autophagy in atheroprotection. Defective autophagy is associated with pro-atherogenic inflammasome activation. Classic inflammasome markers were robustly induced in ATG5-null mϕ, especially when co-incubated with cholesterol crystals. Moreover, cholesterol crystals appear to be increased in ATG5-mϕKO plaques, suggesting a potentially vicious cycle of crystal formation and inflammasome activation in autophagy-deficient plaques. These results show that autophagy becomes dysfunctional in atherosclerosis and its deficiency promotes atherosclerosis in part through inflammasome hyperactivation.

INTRODUCTION

Autophagy is the mechanism by which cytoplasmic components such as organelles and protein aggregates are broken down and recycled via the lysosomal apparatus (reviewed in (Kundu and Thompson, 2008)). During periods of starvation, autophagy promotes survival

Correspondence: csemenko@wustl.edu.

by degrading the cytoplasm in bulk, whereas during nutrient excess, autophagy acts to selectively remove damaged organelles (Klionsky and Emr, 2000; Kundu and Thompson, 2008). This process is highly evolutionarily conserved, but mammalian organisms have also adapted autophagy for more diverse uses such as clearance of pathogens and coordination with apoptosis (Levine et al., 2011; Maiuri et al., 2007). Autophagy is relevant to human disease. Defects in autophagy have been implicated in the pathogenesis of cancers, neurodegenerative diseases, heart failure, and inflammatory bowel disease (Komatsu et al., 2006; Kundu and Thompson, 2008; Levine and Kroemer, 2008; Levine et al., 2011; Nakai et al., 2007). Little is known about the role of autophagy in atherosclerosis.

Limited evidence indicates that autophagy occurs in atherosclerosis, an expected finding given the presence of autophagic markers in most organ systems. Transmission electron microscopy images of atherosclerotic plaques reveals structures consistent with autophagosomes (Kockx et al., 1998; Martinet and De Meyer, 2009) and certain marker proteins of autophagy have been detected in atherosclerotic plaques by immunoblot or immunohistochemical analysis (Martinet et al., 2004; Martinet and De Meyer, 2009). The degree to which autophagy occurs in plaque development, which cells in the atheroma contribute to this process, and whether autophagy impacts lesion formation are unknown. Here, we address these issues using animals with experimental atherosclerosis, ApoE-null mice. We found that while most cells of the plaque have autophagic markers, macrophages appear to be most active at this process, and that autophagy becomes dysfunctional with plaque progression. We show that complete disruption of macrophage autophagy, but not partial disruption, increases plaque formation. Mechanistically, this process in part involves hyperactivation of the macrophage inflammasome and excess IL-1β production. In the autophagy-deficient setting, cholesterol crystals, a hallmark of atherosclerotic plaques, become potent stimuli for inflammasome activation.

RESULTS

Progressive Atherosclerosis Has Features of Dysfunctional Autophagy

Autophagy is dynamic with autophagosome formation, cargo sequestration, and eventual lysosomal fusion/degradation occurring in rapid succession. Not surprisingly, there are no ideal techniques for assessing autophagy flux *in vivo* (Klionsky et al., 2008). However, p62/SQSTM1, a chaperone that shuttles intracellular protein aggregates into autophagosomes for degradation, has emerged as a useful marker of autophagic status (Bjorkoy et al., 2005; Klionsky et al., 2008; Komatsu et al., 2007; Mathew et al., 2009). Since the entire p62/SQSTM1-protein aggregate complex is degraded after engulfment by the autolysosome, p62/SQSTM1 levels are inversely correlated with autophagic flux, i.e. increases in p62/SQSTM1 indicate defective autophagy (Komatsu et al., 2007; Mathew et al., 2009). We fed ApoE-null mice (known to be atherosclerosis susceptible) and their wild type counterparts (with normal ApoE alleles, no defects in cholesterol metabolism, and thus atherosclerosis resistant) a Western diet for 2 months and assessed p62 levels in aortic lysates. p62 protein was dramatically increased in atherosclerotic aortas (Figure 1A), consistent with the presence of defective autophagy. Levels of p62 mRNA were not significantly increased in atherosclerotic aortas and prolonged fasting (a known stimulus for induction of autophagy) of these mice resulted in decreased levels of p62 protein in atherosclerotic aortas (data not shown), suggesting that changes in aortic p62 protein reflect in vivo autophagy status. To determine how plaque progression affects autophagy, we prepared aortic lysates from ApoE-null mice over time since atherosclerosis progresses with age in this model. p62 levels rise with increasing age/plaque burden (Figure 1B). Protein levels of Beclin-1, a component of the complex involved in initial nucleation/formation of the autophagosome (Levine and Kroemer, 2008), were not significantly different in these lysates (Figure 1A,B), suggesting

that any observed autophagy effects in atherosclerosis might involve downstream components of the autophagic pathway.

To determine which cells in atherosclerotic plaques express autophagy markers, we characterized ApoE-null atherosclerotic aortic roots by immunofluorescence. The autophagy markers p62 (Figure 1C) and LC3/ATG8 (Figure 1D) were concurrently imaged with MOMA-2 (an antibody that recognizes monocyte-macrophages), an antibody to CD11b (expressed predominantly on monocyte-macrophages), an antibody to α-smooth muscle cell actin (specific for smooth muscle cells), or an antibody directed to the pan-leukocyte marker CD45. Both p62 and LC3/ATG8 co-localize with plaque leukocytes (Figure 1C, D lower right panels) that are mostly of the monocyte-macrophage macrophage lineage, i.e. MOMA-2 or CD11b positive cells (Figure 1C, D left panels). Smooth muscle cells constitute a small portion of these early atherosclerotic lesions and do not appear to contribute significantly to the autophagic process (Figure 1C, D upper right panels). These results suggest that monocyte/macrophages are the predominant cell type expressing autophagy markers in the plaque and are likely responsible for progressive autophagy deficiency.

Autophagy Haploinsufficiency Has No Effect on Plaque Progression

To perturb autophagy in atherosclerosis, we first used Beclin-1/ATG6 heterozygous-deficient (also known as Beclin-Het) mice. These animals are haploinsufficient for autophagy in numerous organ systems and have been used to assess the function of autophagy in cancer and heart failure (Qu et al., 2003; Yue et al., 2003; Zhu et al., 2007). Beclin-Het mice and their control counterparts each on the ApoE-null background were fed a Western diet for two months. Protein levels of p62 were increased in aortic lysates from Beclin-Hets confirming deficiency in plaque autophagy (Figure 2A). There was no genotype-specific effect on body weight, serum lipids, or insulin sensitivity as gauged by glucose and insulin tolerance tests (Supplemental Figure 1A,B,C). Surprisingly, the presence of a partial autophagy defect in the Beclin-Het/ApoE null animals did not affect the extent of atherosclerosis assayed at the aortic root (Figure 2B) or in the whole aorta *en face* (Figure 2C) as compared to ApoE null animals that were wild type at the Beclin locus.

Complete Deficiency of Macrophage Autophagy Is Pro-inflammatory

One interpretation of the lack of effect of Beclin haploinsufficency on atherosclerosis is that the autophagy defect in this model is inadequate to impact atheroma progression. To pursue this notion, we compared macrophages from Beclin-Het mice with those from macrophage-specific ATG5-null (ATG5-mϕKO) mice, cells with complete absence of an autophagy gene. ATG5-null mϕ *in vitro* had the expected absence of ATG5 in concert with dramatic increases in p62 levels and a loss of the lipidated-LC3 band, both characteristic of complete autophagy deficiency (Figure 3A).

The significant degree of autophagy deficiency in ATG5-null mϕ also manifested itself functionally. After stimulation with LPS, ATG5-null macrophages selectively secreted IL-1β, but not TNF-α, at levels considerably greater than control macrophages (Figure 3B). In contrast, Beclin-Het macrophages failed to secrete either cytokine at levels different from control macrophages (Figure 3C). This *in vitro* pro-inflammatory phenotype was recapitulated *in vivo* since macrophage-specific ATG5-null mice (ATG5-mϕKO) robustly produced serum IL-1β in response to LPS injection (Figure 3D). Even in the absence of LPS stimulation, serum IL-1β levels were increased in ATG5-mϕKO/ApoE-null mice fed a Western diet for two months as compared to similarly treated ApoE null mice with normal levels of macrophage ATG5 (Figure 3E). Other classic pro-inflammatory (TNFα) and anti-inflammatory (IL-10) cytokines were not altered in the serum (Supplemental Figure 2),

suggesting that ATG5 deficiency promotes a specific pro-inflammatory state with metabolic stress. ATG16L1-null macrophages, another model of autophagy deficiency, also selectively hypersecrete IL-1β in response to LPS (Saitoh et al., 2008).

Complete Deficiency of Macrophage Autophagy Enhances Plaque Progression

To determine if the absence of macrophage autophagy affects atherosclerosis, we fed a Western diet for two months to ATG5-mϕKO mice and control mice carrying ATG5 floxed alleles in the absence of the Cre transgene each on an ApoE-null background. p62 levels were increased in the vasculature of the ATG5-mϕKO animals consistent with deficient plaque autophagy (Figure 4A). There was no genotype-specific effect on body weight, serum lipids, or insulin sensitivity (Supplemental Figure 3A,B,C). However, atherosclerotic lesions were increased in ATG5-mϕKO compared to controls as assayed by both aortic root and whole aorta *en face* techniques (Figure 4B,C).

The increased Oil Red O staining seen in ATG5-mϕKO lesions (Figure 4B) suggested an increase in foam cells, usually of macrophage origin. Indeed, staining aortic roots with MOMA-2 revealed a significant portion of the ATG5-mϕKO plaque area is composed of macrophages (data not shown). These observations are supported by a recent report demonstrating a role for autophagy in cholesterol efflux and foam cell formation (Ouimet et al., 2011). In this regard, we also observed a reduced capacity for cholesterol efflux in ATG5-mϕKO macrophages (Figure 4D). Given the pro-inflammatory phenotype of ATG5-mϕKO macrophages, we also assessed the degree of IL-1β in atherosclerotic aortas from control and ATG5-mϕKO animals. After two months of Western diet feeding, a pro-atherogenic intervention leading to overt plaque formation, IL-1β levels were markedly elevated in ATG5-mϕKO aortas (Figure 4E). In contrast, with chow diet feeding, a condition under which atherogenesis is blunted, IL-1β levels were not significantly altered (Figure 4F). Moreover, aortic p62 levels were not significantly elevated on a chow diet (Figure 4G), supporting the notion that autophagy deficiency in plaques is associated with progressive macrophage infiltration and atherogenesis.

Autophagy Deficiency Leads to Hyperactivation of the Macrophage Inflammasome

To understand the mechanistic basis of increased atherosclerosis in ATG5-mϕKO mice, we returned to the pro-inflammatory phenotype of the macrophages in these animals. The hypersecretion of IL-1β in response to LPS (Figure 3B) by ATG5-null macrophages does not occur due to transcriptional effects since message levels for IL-1β and TNF-α respond similarly to LPS in ATG5-null and control macrophages (Supplemental Figure 4). IL-1β protein is processed from a precursor form to a mature, secreted form through activation of caspase-1, the major effector of inflammasome action (Davis et al., 2011; Schroder et al., 2010). Thus, selective hypersecretion of IL-1β is characteristic of inflammasome activation. Similar levels of pro-IL-1β were present in cell lysates from both ATG5-null and control macrophages after LPS treatment (Figure 5A, upper panels), but ATG5-null macrophages hypersecrete the active/truncated forms of both IL-1β and the caspase-1 p10 subunit (Figure 5A, lower panels). Therefore, defects in autophagy due to ATG5 deficiency produce inflammasome hyperactivation resembling findings with defects in autophagy due to ATG16L1 deficiency (Saitoh et al., 2008).

Inflammasome activation may be critical for atheroma progression, various forms of crystalline/particulate materials are potent stimuli for inflammasome activation, and recent findings indicate that cholesterol crystals, a hallmark of atherosclerotic plaques, trigger this process (Duewell et al., 2010; Rajamaki et al., 2010). Treatment of ATG5-null macrophages with a combination of LPS and cholesterol crystals induced IL-1β secretion to levels several-fold higher than LPS alone (Figure 5B). Cholesterol crystal addition did not affect

the phenotypic appearance of macrophages in these experiments (not shown). To confirm that such robust secretion of IL-1β in the setting of autophagy deficiency was primarily an inflammasome-dependent process, we conducted a series of complementary experiments. Although LPS increases the transcription of certain components of the inflammasome, the transcriptional response is not altered in the setting of autophagy deficiency (Supplemental Figure 5). Stimulation of ATG5-null macrophages with LPS and cholesterol crystals leads to increased formation of Apoptotic Speck Protein bodies (ASC "specks") (Figure 5C), a hallmark of inflammasome complex formation and activation (Huang et al., 2009). Macrophages from macrophage-specific ATG7-null mice, an independent model of autophagy-deficiency have similarly elevated IL-1β responses to LPS and cholesterol crystals (Figure 5D). Chemical inhibition of Caspase-1, the downstream effector of inflammasome activation, blunts IL-1β responses in macrophages (Figure 5E). Similarly, macrophages lacking either NLRP3 or ASC, the primary components of the inflammasome complex, have a highly diminished capacity to secrete IL-1β (Figure 5F).

Conversely, although induction of autophagy has been reported to reduce IL-1β (Harris et al., 2011), this effect appears to be independent of inflammasomes since induction of autophagy in macrophages through nutrient depletion decreases cellular levels of both pro- and mature forms of IL-1β in concert with reducing its secretion (Supplemental Figure 6). This result, using peritoneal macrophages and confirming the findings of Harris et al. (2011), was limited to induction of autophagy. In a different model system, bone marrow-derived macrophages, induction of autophagy in combination with the NLRP3 agonist nigericin promotes the unconventional secretion of IL-1β (Dupont et al., 2011). These data suggest that the effects of temporally discrete induction of autophagy on IL-1β responses are complex and context-dependent. However, our results indicate that defective basal autophagy in mice with ATG5-null macrophages increases atherosclerosis and aortic IL-1β levels in a manner that appears to involve the inflammasome.

Potential Mediators of Atherosclerotic Progression

Cholesterol crystals are a significant component of atherosclerotic plaques and are also detectable in early lesions (Duewell et al., 2010). Cholesterol crystal area as determined by reflectance microscopy was increased in ATG5-mϕKO atherosclerotic lesions (Figure 6A). One interpretation of this finding is that the pro-inflammatory state of ATG5-null macrophages may be perpetuated by the increased cholesterol crystal burden of atherosclerotic plaques. Extracellular cholesterol crystals are initially trafficked to the lysosomal compartment of the macrophage where they are inefficiently and partially dissolved for downstream reesterification (Duewell et al., 2010; Kruth et al., 1995; Rajamaki et al., 2010). Persistently undissolved crystals remain trapped in the lysosomal compartment where they may render the lysosome and processes such as autophagy dysfunctional (Duewell et al., 2010; Rajamaki et al., 2010). Indeed, macrophages incubated with cholesterol crystals over a 12 hour period show concomitant increases in p62 levels and increased conversion of LC3-I to LC3-II, suggesting that although some components of the autophagic process are not affected, the final fusion/degradation step with the lysosome is impaired (Figure 6B). Thus, cholesterol crystals have the ability to incite inflammasome activation as well as block autophagic processing.

One of the proposed mechanisms for inflammasome activation has been the presence of reactive oxygen species (ROS) (Gross et al., 2011; Naik and Dixit, 2011). Thus, we looked for signatures of ROS activation in the ATG5-mϕKO atherosclerotic plaques. Protein carbonylation, a marker of increased oxidative modification of proteins (Stadtman, 1993), was significantly elevated in atherosclerotic ATG5-mϕKO aortas as assessed by Western blot analysis (Figure 6C). Similarly, dihydroethidium (DHE) staining of atherosclerotic

aortic roots, a measure of intracellular superoxide levels, was increased in ATG5-mϕKO plaques (Figure 6D).

DISCUSSION

In this study, we provide evidence supporting a role for defective autophagy in the pathogenesis of atherosclerosis. Progressive plaque formation has features of defective autophagy predominantly related to plaque macrophages. A modest decrease in plaque autophagy (Beclin-Het model) does not affect experimental atherosclerosis but the loss of macrophage autophagy (ATG5-mϕKO model) accelerates atheroma progression. The autophagy-deficient setting appears to exacerbate a cholesterol crystal-mediated hyperactivation of the macrophage inflammasome with its pro-atherogenic IL-1β response. Links between autophagy, the inflammasome, and atherogenesis are summarized in Figure 7.

Atherosclerosis is complex and our understanding of the biology of proteins such as ATG5 is evolving. It is possible that autophagy-independent roles of ATG5 might be involved in the atherosclerotic phenotype of the ATG5-mϕKO mice. However, inflammasomes are involved in atherosclerosis (Duewell et al., 2010), IL-1β secretion may indicate inflammasome activation (Davis et al., 2011), and deficiencies of three distinct autophagy proteins--ATG16L1 (Saitoh et al., 2008), ATG5 (Figure 5B) and ATG7 (Figure 5D), are associated with increased IL-1β secretion. Collectively, these findings support the notion that autophagy deficiency promotes atherosclerosis.

Cholesterol crystals, characteristic of atherosclerotic plaques, activate inflammasomes, providing a mechanistic basis for propagating atherogenesis (Duewell et al., 2010; Masters et al., 2011). Our results indicate that intact autophagy suppresses the inflammasome, but the nature of this suppression is unclear. One potential mechanism could involve the autophagic removal of damaged mitochondria (also called mitophagy), in turn reducing reactive oxygen species (ROS) production. Release of ROS and DNA from damaged mitochondria can activate inflammasomes, a process that is exacerbated in the absence of mitophagy (Naik and Dixit, 2011; Nakahira et al.; Zhou et al., 2011). The observation that ATG5-mϕKO plaques have increased markers of protein oxidation and superoxide production lends credence to this possibility. Also consistent with this notion, the saturated fatty acid palmitate appears to inhibit autophagy while also increasing mitochondrial ROS to induce inflammasome activation (Wen et al., 2011).

A second potential mechanism could involve the removal of dysfunctional lysosomes (so-called lysosomophagy) (Klionsky et al., 2007). Lysosomal destabilization, which promotes inflammasome activation, has been reported when poorly digestible extracellular particulate matter (including cholesterol crystals) is phagocytosed and shuttled to lysosomes for degradation (Duewell et al., 2010; Hornung et al., 2008; Masters et al., 2011). The pro-inflammatory nature of these dysfunctional lysosomes can be accentuated in the absence of lysosomophagy. Additionally, evidence that cholesterol crystals affect the progression of autophagy at the level of the lysosome serves to further exacerbate this process. Given the broad range of organelles and cellular components cleared by autophagy, pleiotropic mechanisms may be coordinately activating the inflammasome in the setting of defective autophagy.

What degree of autophagy-deficiency is pro-atherogenic? The difference in phenotypes between the Beclin-Het and ATG5-mϕKO mice suggests that promotion of atherosclerosis requires considerable disruption of constitutive plaque autophagy. However, autophagy deficient states in humans would be expected to be incompatible with life: all animal models

of whole-body autophagy deficiencies described to date are either embryonically or neonatally lethal (Komatsu et al., 2005; Kuma et al., 2004; Saitoh et al., 2008). If, as suggested by our results with Beclin-Het animals, autophagy heterozygosity in humans is not pro-atherogenic, severe defects in autophagy would have to be acquired in order to impact human vascular disease.

Published evidence supports this possibility. Cells in atherosclerotic plaques develop progressive lysosomal dysfunction with features resembling a lysosomal storage disease (Jerome, 2006). The accumulation of unhydrolyzed cholesteryl esters and trapped/poorly translocated free cholesterol in lysosomes has been described in macrophage foam cells (Brown et al., 2000; Dhaliwal and Steinbrecher, 2000; Griffin et al., 2005; Jessup et al., 1992; Lougheed et al., 1991; Yancey and Jerome, 2001). These unmetabolized substituents may impair the lysosomal degradation capacity of lipases as well as other enzymes including proteases. Our observation that p62 accumulates in advanced atherosclerotic plaques is consistent with this concept.

If acquired defects in plaque autophagy exacerbate atherosclerosis, inducing autophagy might be anti-atherogenic. No studies have addressed this notion directly. However, sirolimus and everolimus, both inhibitors of the autophagy-suppressing kinase mTOR and thus classic stimulators of autophagy, are anti-atherogenic in mice (Castro et al., 2004; Mueller et al., 2008; Pakala et al., 2005; Zhao et al., 2009). Calorie-restricted mice, another stimulus for autophagy induction (Wohlgemuth et al., 2007), also have reduced atherosclerosis (Guo et al., 2002).

Atherosclerosis has been documented in humans who lived ~1500 BCE (Allam et al., 2009), when epidemic obesity and highly processed, nutrient-dense foods did not exist. Egyptian scholars attributed vascular disease to “wekhedu”, undigested food that accumulated in the vasculature to limit blood flow and promote disease. Since deficient autophagy reflects an inability to digest cellular food, our findings suggest that ancient scientists may have been at least partially correct.

EXPERIMENTAL PROCEDURES

Animals

Protocols were approved by the Washington University Animal Studies Committee. Beclin +/− (Beclin-Het) mice, a gift from Dr. Nathaniel Heintz, Rockefeller University (Yue et al., 2003), were backcrossed with ApoE−/− mice (C57BL/6 background) to generate Beclin+/−ApoE null and Beclin+/+ApoE null littermates used for experiments that were >N7 C57BL/6. Mice with the floxed ATG5 locus, a gift from Dr. Noboru Mizushima, Tokyo Medical & Dental University (Hara et al., 2006), were crossed with Cre-recombinase transgenic mice under the control of the Lysosomal-M promoter and ApoE−/− mice to generate mice with macrophage-specific ATG5 deficiency and littermate controls that were >N7 C57BL/6. Beclin, ATG5, Cre, and ApoE genotyping was performed as previously described (Chakravarthy et al., 2005; Hara et al., 2006; Yue et al., 2003). $ATG7^{flox/flox}$, NLRP3−/−, and ASC−/− mice have been previously described (Hara et al., 2006; Mariathasan et al., 2004; Sutterwala et al., 2006). Mice housed in a specific pathogen-free barrier facility were weaned at 3 weeks of age to a standard mouse chow providing 6% calories as fat, then started on a Western-type diet containing 0.15% cholesterol providing 42% calories as fat (TD 88137, Harlan, Madison, WI) at ~8 weeks of age.

Analytical Procedures and Lesion Quantification

Serum IL-1β, whole aorta IL-1β, and secreted IL-1β and TNF-α from culture media were measured using ELISA assays from R&D Systems Inc (MLB00B) and BD Biosciences

Pharmingen (559732). Cholesterol, triglycerides, glucose and free (nonesterified) fatty acids (FFA) were assayed in serum following a 4-hour fast as described (Li et al., 2000). Glucose tolerance and insulin tolerance tests (GTT and ITT) were separated by at least a week using fasted mice that were injected with 10% D-glucose (1 g/kg) or human regular insulin (0.75 units/kg body weight, Eli Lilly and Co., Indianapolis, IN). Tail vein blood for these tests was assayed at 0, 30, 60, and 120 min using a glucose meter (Contour, Bayer Healthcare, Mishawaka, IN). Serum TNF-α and IL-10 were measured using ELISA assays from BD Biosciences Pharmingen (559732) and R&D Systems Inc (M1000). For assessment of IL-1β, TNFα, NLRP3, ASC, and Caspase-1 transcript levels, extraction of total RNA, reverse transcription, and quantitative RT-PCR were performed as described (Razani et al., 2011). Sequences for the oligonucleotide primers used were designed using the qPrimerDepot database-http://primerdepot.nci.nih.gov. Assays were performed in duplicate and normalized to amplified mRNA for ribosomal protein L32.

The *en face* and aortic root cross-section techniques previously described (Semenkovich et al., 1998) were used to quantify atherosclerosis throughout the aorta as well as at the vessel origin. *En face* regions were analyzed as the aortic arch (from the aortic valve to the left subclavian artery), thoracic aorta (from the left subclavian artery to the final intercostal arteries), and abdominal aorta (from the intercostal arteries to the bifurcation of the iliac arteries).

Macrophage Culture and Inflammasome Stimulation

Macrophages were isolated essentially as described (Febbraio et al., 2000) by injecting mice intraperitoneally with a 4% solution of thioglycollate media (Sigma, St. Louis, MO) on day 1. On day 5, peritoneal macrophages were isolated, washed, counted, and plated in DMEM with 10% FBS. Macrophages were subsequently harvested at various times to isolate protein using standard techniques. Cholesterol crystals were generated by subjecting cholesterol powder (Sigma, St. Louis, MO) to an ethanol precipitation technique as described (Rajamaki et al., 2010; Whiting and Watts, 1983). Time-course stimulation with LPS (Sigma, St. Louis, MO) with or without cholesterol crystals was performed as indicated in the respective figure legends. Chemical inhibition of inflammasomes was performed with 10 mM Caspase-1 inhibitor Z-YVAD-FMK (Enzo Life Sciences, Farmingdale, NY).

Cholesterol Efflux

Experiments were performed as described with some modifications (Schneider et al., 2010). Briefly, ^{3}H-labeled AcLDL was made by incubating AcLDL (Invitrogen - 100 μg/ml) with ^{3}H-cholesterol (American Radiolabel Chemical - 2.5 μCi/ml) for 24 hours. Macrophages were labeled with ^{3}H-labeled AcLDL for 24 hours, equilibrated in 0.2% BSA for 12 hours, and incubated in the presence or absence of ApoAI (Invitrogen - 25 μg/ml) for an 8, 24, and 48 hour time-course. The ApoAI-dependent cholesterol efflux was determined as a percentage of ^{3}H-cholesterol in the media relative to total ^{3}H-cholesterol in the media and cells.

Western Blotting

Separation, transfer and blotting were performed as described (Razani et al., 2001) using the following antibodies: p62/SQSTM1 (610832) from BD Biosciences, San Diego, CA; β-actin (A2066) from Sigma-Aldrich Corp., St. Louis, MO; Beclin-1 (H-300) and Caspase-1 p10 (M-20) from Santa Cruz Biotechnology Inc., Santa Cruz, CA; LC3/ATG8 (NB100-2220) and ATG5 (NB110-53818) from Novus Biologicals Inc., Littleton, CO; and IL-1β (AF-401-NA) from R&D Systems Inc., Minneapolis, MN. Detection of protein oxidation by Western blotting was performed using the OxyBlot™ Kit (Millipore, Billerica, MA) per manufacturer's instructions.

Microscopy

Immunofluorescence microscopy of frozen-tissue sections and paraformaldehyde-fixed macrophages was performed as previously described (Razani et al., 2001). Studies included parallel experiments omitting primary or secondary antibodies to validate specificity of the images. The following primary antibodies were used: p62/SQSTM1 (GP62) from Progen Biotechnik BmbH, Heidelberg, Germany; LC3/ATG8 (#2775) from Cell Signaling Technology Inc., Danvers, MA; MOMA-2 (MCA519G) from AbD Serotec, Oxford, UK; α-smooth muscle actin (1A4 – FITC conjugate) from Sigma-Aldrich Corp., St. Louis, MO; CD11b (14-0112) and CD45 (14-0451) from eBioscience Inc., San Diego, CA; and ASC (AL177) from Enzo Life Sciences, Inc., Plymouth Meeting, PA. Species-specific fluoroprobe-conjugated secondary antibodies were obtained from Invitrogen Corp., Carlsbad, CA. Imaging of cholesterol crystals was performed using reflectance microscopy (Zeiss LSM 510 confocal laser-scanning microscope) essentially as previously described (Duewell et al., 2010). Crystal area quantification was performed with ImageJ software (imagej.nih.gov). Assessment of oxidative stress in aortic root frozen-tissue sections was performed by fluorescence microscopy of dihydroethidium (DHE) stained sections as previously described (Michel et al., 2011).

Statistical Analyses

Statistical significance of differences was calculated using the Student unpaired t test for parametric data (*in vitro* macrophage experiments and serum metabolites; GTT and ITT results) or the Mann-Whitney test for nonparametric data (atherosclerosis and cholesterol crystal quantitation). Graphs containing error bars show the mean ± standard error of the mean (SEM).

HIGHLIGHTS

- Atherosclerotic plaques have features of defective mϕ autophagy
- Complete deficiency of mϕ autophagy increases atherosclerosis
- Loss of mϕ autophagy leads to hyperactivation of inflammasomes and IL-1β release
- Cholesterol crystals exacerbate inflammasome activation in autophagy deficiency

Supplementary Material

Refer to Web version on PubMed Central for supplementary material.

Acknowledgments

This work was supported by HL083762, DK076729, DK088083, DK56341 (CNRU), DK20579 (DRTC), 5K08HL098559, as well as the Physician Scientist Training Program and Cardiovascular Training Grant at Washington University. We thank Tony Pryse of the Washington University Fluorescence Correlation Spectroscopy and Confocal Imaging Facility for technical assistance with reflectance microscopy, Kenneth Caldwell and Brian Miller for assistance with autophagy reagents, and Christopher Holley, Benjamin Scruggs, Joel Schilling, and Jean Schaffer for help with assessing reactive oxygen species.

REFERENCES

Allam AH, Thompson RC, Wann LS, Miyamoto MI, Thomas GS. Computed tomographic assessment of atherosclerosis in ancient Egyptian mummies. JAMA. 2009; 302:2091–2094. [PubMed: 19920233]

Bjorkoy G, Lamark T, Brech A, Outzen H, Perander M, Overvatn A, Stenmark H, Johansen T. p62/SQSTM1 forms protein aggregates degraded by autophagy and has a protective effect on huntingtin-induced cell death. J Cell Biol. 2005; 171:603–614. [PubMed: 16286508]

Brown AJ, Mander EL, Gelissen IC, Kritharides L, Dean RT, Jessup W. Cholesterol and oxysterol metabolism and subcellular distribution in macrophage foam cells. Accumulation of oxidized esters in lysosomes. J Lipid Res. 2000; 41:226–237. [PubMed: 10681406]

Castro C, Campistol JM, Sancho D, Sanchez-Madrid F, Casals E, Andres V. Rapamycin attenuates atherosclerosis induced by dietary cholesterol in apolipoprotein-deficient mice through a p27 Kip1 - independent pathway. Atherosclerosis. 2004; 172:31–38. [PubMed: 14709354]

Chakravarthy MV, Pan Z, Zhu Y, Tordjman K, Schneider JG, Coleman T, Turk J, Semenkovich CF. "New" hepatic fat activates PPARalpha to maintain glucose, lipid, and cholesterol homeostasis. Cell Metab. 2005; 1:309–322. [PubMed: 16054078]

Davis BK, Wen H, Ting JP. The inflammasome NLRs in immunity, inflammation, and associated diseases. Annu Rev Immunol. 2011; 29:707–735. [PubMed: 21219188]

Dhaliwal BS, Steinbrecher UP. Cholesterol delivered to macrophages by oxidized low density lipoprotein is sequestered in lysosomes and fails to efflux normally. J Lipid Res. 2000; 41:1658–1665. [PubMed: 11013308]

Duewell P, Kono H, Rayner KJ, Sirois CM, Vladimer G, Bauernfeind FG, Abela GS, Franchi L, Nunez G, Schnurr M, et al. NLRP3 inflammasomes are required for atherogenesis and activated by cholesterol crystals. Nature. 2010; 464:1357–1361. [PubMed: 20428172]

Dupont N, Jiang S, Pilli M, Ornatowski W, Bhattacharya D, Deretic V. Autophagy-based unconventional secretory pathway for extracellular delivery of IL-1β. EMBO J. 2011; 30:4701–4711. [PubMed: 22068051]

Febbraio M, Podrez EA, Smith JD, Hajjar DP, Hazen SL, Hoff HF, Sharma K, Silverstein RL. Targeted disruption of the class B scavenger receptor CD36 protects against atherosclerotic lesion development in mice. J Clin Invest. 2000; 105:1049–1056. [PubMed: 10772649]

Griffin EE, Ullery JC, Cox BE, Jerome WG. Aggregated LDL and lipid dispersions induce lysosomal cholesteryl ester accumulation in macrophage foam cells. J Lipid Res. 2005; 46:2052–2060. [PubMed: 16024919]

Gross O, Thomas CJ, Guarda G, Tschopp J. The inflammasome: an integrated view. Immunol Rev. 2011; 243:136–151. [PubMed: 21884173]

Guo Z, Mitchell-Raymundo F, Yang H, Ikeno Y, Nelson J, Diaz V, Richardson A, Reddick R. Dietary restriction reduces atherosclerosis and oxidative stress in the aorta of apolipoprotein E-deficient mice. Mech Ageing Dev. 2002; 123:1121–1131. [PubMed: 12044962]

Hara T, Nakamura K, Matsui M, Yamamoto A, Nakahara Y, Suzuki-Migishima R, Yokoyama M, Mishima K, Saito I, Okano H, et al. Suppression of basal autophagy in neural cells causes neurodegenerative disease in mice. Nature. 2006; 441:885–889. [PubMed: 16625204]

Harris J, Hartman M, Roche C, Zeng SG, O'Shea A, Sharp FA, Lambe EM, Creagh EM, Golenbock DT, Tschopp J, et al. Autophagy controls IL-1beta secretion by targeting pro-IL-1beta for degradation. J Biol Chem. 2011; 286:9587–9597. [PubMed: 21228274]

Hornung V, Bauernfeind F, Halle A, Samstad EO, Kono H, Rock KL, Fitzgerald KA, Latz E. Silica crystals and aluminum salts activate the NALP3 inflammasome through phagosomal destabilization. Nat Immunol. 2008; 9:847–856. [PubMed: 18604214]

Huang MT, Taxman DJ, Holley-Guthrie EA, Moore CB, Willingham SB, Madden V, Parsons RK, Featherstone GL, Arnold RR, O'Connor BP, et al. Critical role of apoptotic speck protein containing a caspase recruitment domain (ASC) and NLRP3 in causing necrosis and ASC speck formation induced by Porphyromonas gingivalis in human cells. J Immunol. 2009; 182:2395–2404. [PubMed: 19201894]

Jerome WG. Advanced atherosclerotic foam cell formation has features of an acquired lysosomal storage disorder. Rejuvenation Res. 2006; 9:245–255. [PubMed: 16706652]

Jessup W, Mander EL, Dean RT. The intracellular storage and turnover of apolipoprotein B of oxidized LDL in macrophages. Biochim Biophys Acta. 1992; 1126:167–177. [PubMed: 1627619]

Klionsky DJ, Abeliovich H, Agostinis P, Agrawal DK, Aliev G, Askew DS, Baba M, Baehrecke EH, Bahr BA, Ballabio A, et al. Guidelines for the use and interpretation of assays for monitoring autophagy in higher eukaryotes. Autophagy. 2008; 4:151–175. [PubMed: 18188003]

Klionsky DJ, Cuervo AM, Dunn WA Jr, Levine B, van der Klei I, Seglen PO. How shall I eat thee? Autophagy. 2007; 3:413–416. [PubMed: 17568180]

Klionsky DJ, Emr SD. Autophagy as a regulated pathway of cellular degradation. Science. 2000; 290:1717–1721. [PubMed: 11099404]

Kockx MM, De Meyer GR, Buyssens N, Knaapen MW, Bult H, Herman AG. Cell composition, replication, and apoptosis in atherosclerotic plaques after 6 months of cholesterol withdrawal. Circ Res. 1998; 83:378–387. [PubMed: 9721694]

Komatsu M, Waguri S, Chiba T, Murata S, Iwata J, Tanida I, Ueno T, Koike M, Uchiyama Y, Kominami E, et al. Loss of autophagy in the central nervous system causes neurodegeneration in mice. Nature. 2006; 441:880–884. [PubMed: 16625205]

Komatsu M, Waguri S, Koike M, Sou YS, Ueno T, Hara T, Mizushima N, Iwata J, Ezaki J, Murata S, et al. Homeostatic levels of p62 control cytoplasmic inclusion body formation in autophagy-deficient mice. Cell. 2007; 131:1149–1163. [PubMed: 18083104]

Komatsu M, Waguri S, Ueno T, Iwata J, Murata S, Tanida I, Ezaki J, Mizushima N, Ohsumi Y, Uchiyama Y, et al. Impairment of starvation-induced and constitutive autophagy in Atg7-deficient mice. J Cell Biol. 2005; 169:425–434. [PubMed: 15866887]

Kruth HS, Skarlatos SI, Lilly K, Chang J, Ifrim I. Sequestration of acetylated LDL and cholesterol crystals by human monocyte-derived macrophages. J Cell Biol. 1995; 129:133–145. [PubMed: 7698980]

Kuma A, Hatano M, Matsui M, Yamamoto A, Nakaya H, Yoshimori T, Ohsumi Y, Tokuhisa T, Mizushima N. The role of autophagy during the early neonatal starvation period. Nature. 2004; 432:1032–1036. [PubMed: 15525940]

Kundu M, Thompson CB. Autophagy: basic principles and relevance to disease. Annu Rev Pathol. 2008; 3:427–455. [PubMed: 18039129]

Levine B, Kroemer G. Autophagy in the pathogenesis of disease. Cell. 2008; 132:27–42. [PubMed: 18191218]

Levine B, Mizushima N, Virgin HW. Autophagy in immunity and inflammation. Nature. 2011; 469:323–335. [PubMed: 21248839]

Li B, Nolte LA, Ju JS, Han DH, Coleman T, Holloszy JO, Semenkovich CF. Skeletal muscle respiratory uncoupling prevents diet-induced obesity and insulin resistance in mice. Nat Med. 2000; 6:1115–1120. [PubMed: 11017142]

Lougheed M, Zhang HF, Steinbrecher UP. Oxidized low density lipoprotein is resistant to cathepsins and accumulates within macrophages. J Biol Chem. 1991; 266:14519–14525. [PubMed: 1860858]

Maiuri MC, Zalckvar E, Kimchi A, Kroemer G. Self-eating and self-killing: crosstalk between autophagy and apoptosis. Nat Rev Mol Cell Biol. 2007; 8:741–752. [PubMed: 17717517]

Mariathasan S, Newton K, Monack DM, Vucic D, French DM, Lee WP, Roose-Girma M, Erickson S, Dixit VM. Differential activation of the inflammasome by caspase-1 adaptors ASC and Ipaf. Nature. 2004; 430:213–218. [PubMed: 15190255]

Martinet W, De Bie M, Schrijvers DM, De Meyer GR, Herman AG, Kockx MM. 7-ketocholesterol induces protein ubiquitination, myelin figure formation, and light chain 3 processing in vascular smooth muscle cells. Arterioscler Thromb Vasc Biol. 2004; 24:2296–2301. [PubMed: 15458974]

Martinet W, De Meyer GR. Autophagy in atherosclerosis: a cell survival and death phenomenon with therapeutic potential. Circ Res. 2009; 104:304–317. [PubMed: 19213965]

Masters SL, Latz E, O'Neill LA. The inflammasome in atherosclerosis and type 2 diabetes. Sci Transl Med. 2011; 3 81ps17.

Mathew R, Karp CM, Beaudoin B, Vuong N, Chen G, Chen HY, Bray K, Reddy A, Bhanot G, Gelinas C, et al. Autophagy suppresses tumorigenesis through elimination of p62. Cell. 2009; 137:1062–1075. [PubMed: 19524509]

Michel CI, Holley CL, Scruggs BS, Sidhu R, Brookheart RT, Listenberger LL, Behlke MA, Ory DS, Schaffer JE. Small nucleolar RNAs U32a, U33, and U35a are critical mediators of metabolic stress. Cell Metab. 2011; 14:33–44. [PubMed: 21723502]

Mueller MA, Beutner F, Teupser D, Ceglarek U, Thiery J. Prevention of atherosclerosis by the mTOR inhibitor everolimus in LDLR−/− mice despite severe hypercholesterolemia. Atherosclerosis. 2008; 198:39–48. [PubMed: 17980369]

Naik E, Dixit VM. Mitochondrial reactive oxygen species drive proinflammatory cytokine production. J Exp Med. 2011; 208:417–420. [PubMed: 21357740]

Nakahira K, Haspel JA, Rathinam VA, Lee SJ, Dolinay T, Lam HC, Englert JA, Rabinovitch M, Cernadas M, Kim HP, et al. Autophagy proteins regulate innate immune responses by inhibiting the release of mitochondrial DNA mediated by the NALP3 inflammasome. Nat Immunol. 12:222–230. [PubMed: 21151103]

Nakai A, Yamaguchi O, Takeda T, Higuchi Y, Hikoso S, Taniike M, Omiya S, Mizote I, Matsumura Y, Asahi M, et al. The role of autophagy in cardiomyocytes in the basal state and in response to hemodynamic stress. Nat Med. 2007; 13:619–624. [PubMed: 17450150]

Ouimet M, Franklin V, Mak E, Liao X, Tabas I, Marcel YL. Autophagy regulates cholesterol efflux from macrophage foam cells via lysosomal acid lipase. Cell Metab. 2011; 13:655–667. [PubMed: 21641547]

Pakala R, Stabile E, Jang GJ, Clavijo L, Waksman R. Rapamycin attenuates atherosclerotic plaque progression in apolipoprotein E knockout mice: inhibitory effect on monocyte chemotaxis. J Cardiovasc Pharmacol. 2005; 46:481–486. [PubMed: 16160601]

Qu X, Yu J, Bhagat G, Furuya N, Hibshoosh H, Troxel A, Rosen J, Eskelinen EL, Mizushima N, Ohsumi Y, et al. Promotion of tumorigenesis by heterozygous disruption of the beclin 1 autophagy gene. J Clin Invest. 2003; 112:1809–1820. [PubMed: 14638851]

Rajamaki K, Lappalainen J, Oorni K, Valimaki E, Matikainen S, Kovanen PT, Eklund KK. Cholesterol crystals activate the NLRP3 inflammasome in human macrophages: a novel link between cholesterol metabolism and inflammation. PLoS One. 2010; 5:e11765. [PubMed: 20668705]

Razani B, Engelman JA, Wang XB, Schubert W, Zhang XL, Marks CB, Macaluso F, Russell RG, Li M, Pestell RG, et al. Caveolin-1 null mice are viable but show evidence of hyperproliferative and vascular abnormalities. J Biol Chem. 2001; 276:38121–38138. [PubMed: 11457855]

Razani B, Zhang H, Schulze PC, Schilling JD, Verbsky J, Lodhi IJ, Topkara VK, Feng C, Coleman T, Kovacs A, et al. Fatty acid synthase modulates homeostatic responses to myocardial stress. J Biol Chem. 2011; 286:30949–30961. [PubMed: 21757749]

Saitoh T, Fujita N, Jang MH, Uematsu S, Yang BG, Satoh T, Omori H, Noda T, Yamamoto N, Komatsu M, et al. Loss of the autophagy protein Atg16L1 enhances endotoxin-induced IL-1beta production. Nature. 2008; 456:264–268. [PubMed: 18849965]

Schneider JG, Yang Z, Chakravarthy MV, Lodhi IJ, Wei X, Turk J, Semenkovich CF. Macrophage fatty-acid synthase deficiency decreases diet-induced atherosclerosis. J Biol Chem. 2010; 285:23398–23409. [PubMed: 20479009]

Schroder K, Zhou R, Tschopp J. The NLRP3 inflammasome: a sensor for metabolic danger? Science. 2010; 327:296–300. [PubMed: 20075245]

Semenkovich CF, Coleman T, Daugherty A. Effects of heterozygous lipoprotein lipase deficiency on diet-induced atherosclerosis in mice. J Lipid Res. 1998; 39:1141–1151. [PubMed: 9643345]

Stadtman ER. Oxidation of free amino acids and amino acid residues in proteins by radiolysis and by metal-catalyzed reactions. Annu Rev Biochem. 1993; 62:797–821. [PubMed: 8352601]

Sutterwala FS, Ogura Y, Szczepanik M, Lara-Tejero M, Lichtenberger GS, Grant EP, Bertin J, Coyle AJ, Galan JE, Askenase PW, et al. Critical role for NALP3/CIAS1/Cryopyrin in innate and adaptive immunity through its regulation of caspase-1. Immunity. 2006; 24:317–327. [PubMed: 16546100]

Wen H, Gris D, Lei Y, Jha S, Zhang L, Huang MT, Brickey WJ, Ting JP. Fatty acid-induced NLRP3-ASC inflammasome activation interferes with insulin signaling. Nat Immunol. 2011; 12:408–415. [PubMed: 21478880]

Whiting MJ, Watts JM. Cholesterol crystal formation and growth in model bile solutions. J Lipid Res. 1983; 24:861–868. [PubMed: 6631220]

Wohlgemuth SE, Julian D, Akin DE, Fried J, Toscano K, Leeuwenburgh C, Dunn WA Jr. Autophagy in the heart and liver during normal aging and calorie restriction. Rejuvenation Res. 2007; 10:281–292. [PubMed: 17665967]

Yancey PG, Jerome WG. Lysosomal cholesterol derived from mildly oxidized low density lipoprotein is resistant to efflux. J Lipid Res. 2001; 42:317–327. [PubMed: 11254742]

Yue Z, Jin S, Yang C, Levine AJ, Heintz N. Beclin 1, an autophagy gene essential for early embryonic development, is a haploinsufficient tumor suppressor. Proc Natl Acad Sci U S A. 2003; 100:15077–15082. [PubMed: 14657337]

Zhao L, Ding T, Cyrus T, Cheng Y, Tian H, Ma M, Falotico R, Pratico D. Low-dose oral sirolimus reduces atherogenesis, vascular inflammation and modulates plaque composition in mice lacking the LDL receptor. Br J Pharmacol. 2009; 156:774–785. [PubMed: 19220291]

Zhou R, Yazdi AS, Menu P, Tschopp J. A role for mitochondria in NLRP3 inflammasome activation. Nature. 2011; 469:221–225. [PubMed: 21124315]

Zhu H, Tannous P, Johnstone JL, Kong Y, Shelton JM, Richardson JA, Le V, Levine B, Rothermel BA, Hill JA. Cardiac autophagy is a maladaptive response to hemodynamic stress. J Clin Invest. 2007; 117:1782–1793. [PubMed: 17607355]

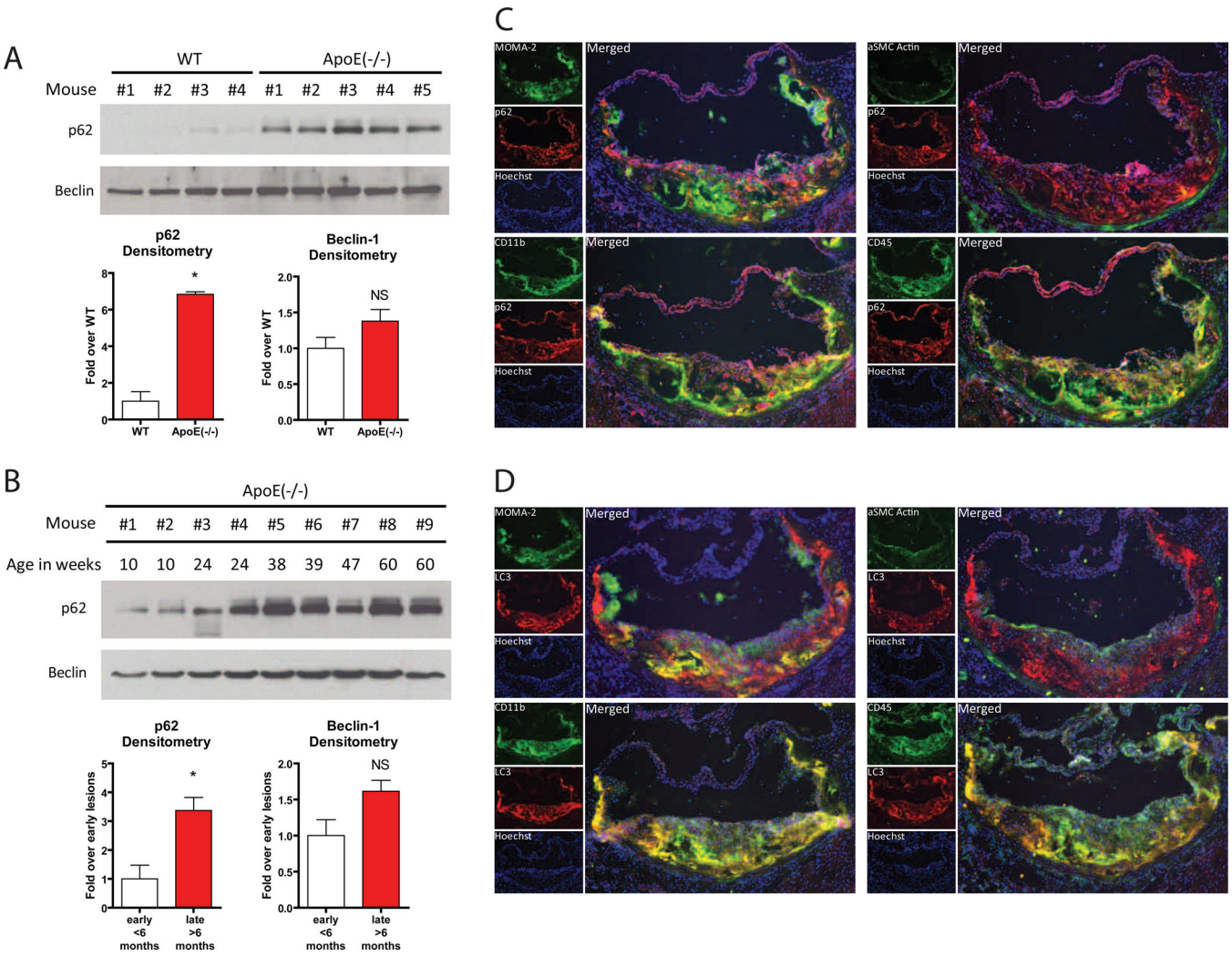

Figure 1. Assessment of Autophagy in the Atherosclerotic Plaque

(A, B) Western blot analysis of p62 and Beclin-1 in whole aorta lysates from (A) wild type (WT, n=4) and ApoE-null (n=5) mice fed a Western diet for 2 months, and (B) ApoE-null mice of increasing age (10 to 60 weeks). Densitometric quantification is shown below each respective Western blot. Data are presented as mean ± SEM. *P<0.05, NS = not significant. (C, D) Immunofluorescence microscopy of aortic root frozen sections from an ApoE-null mouse fed a Western diet for 2 months. (C) In all quadrants, p62 stains (red) and Hoechst-33258 nuclear stains (purple) are shown. Green stains are as follows: MOMA-2 (left upper panel), CD11b (left lower panel), αSMC-Actin (right upper panel), and CD45 (right lower panel). (D) Similar stains to (B) except LC3/ATG8 staining (red) instead of p62. For all panels, smaller individual stains for each protein (labeled) are shown on the left and a larger merged image is shown on the right.

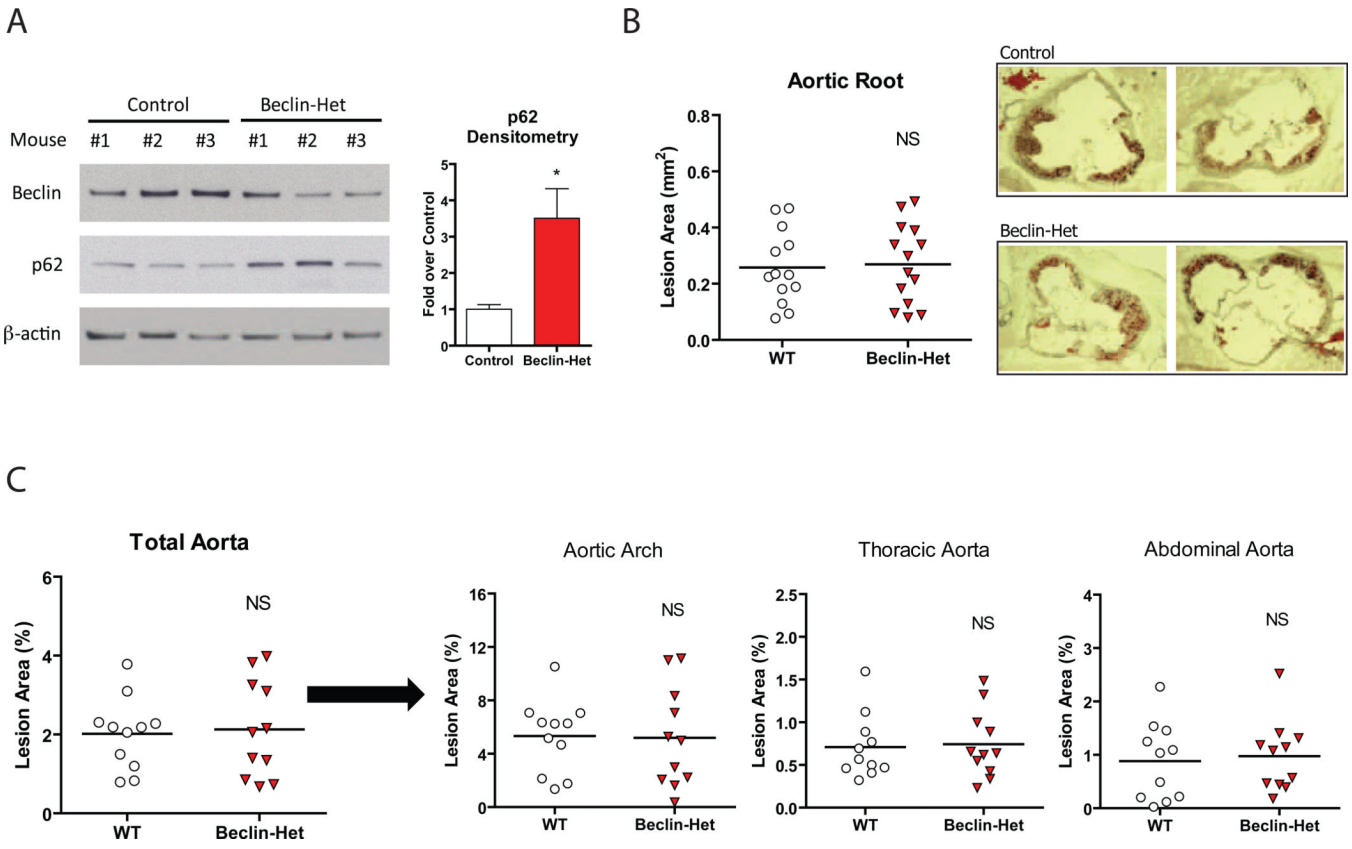

Figure 2. Quantification of Atherosclerosis in the Beclin-Het Autophagy-Deficient Model

(A) Western blot analysis of Beclin-1, p62, and β-actin in whole aorta lysates from control (n=3) and Beclin-Het (n=3) mice each on an ApoE-null background fed a Western diet for 2 months. Densitometric quantification is shown to the right. Data are presented as mean ± SEM. *P<0.05.

(B, C) Cohorts of control and Beclin-Het mice (# of mice shown) were placed on a Western diet for 2 months and atherosclerotic area involvement was determined by computer image analyses.

(B) Oil Red O-stained sections of aortic roots (representative aortic root sections are shown on the right). (C) *En face* results for the total aorta and its regions (aortic arch, thoracic aorta, and abdominal aorta). Horizontal lines within the data sets represent means. NS = not significant.

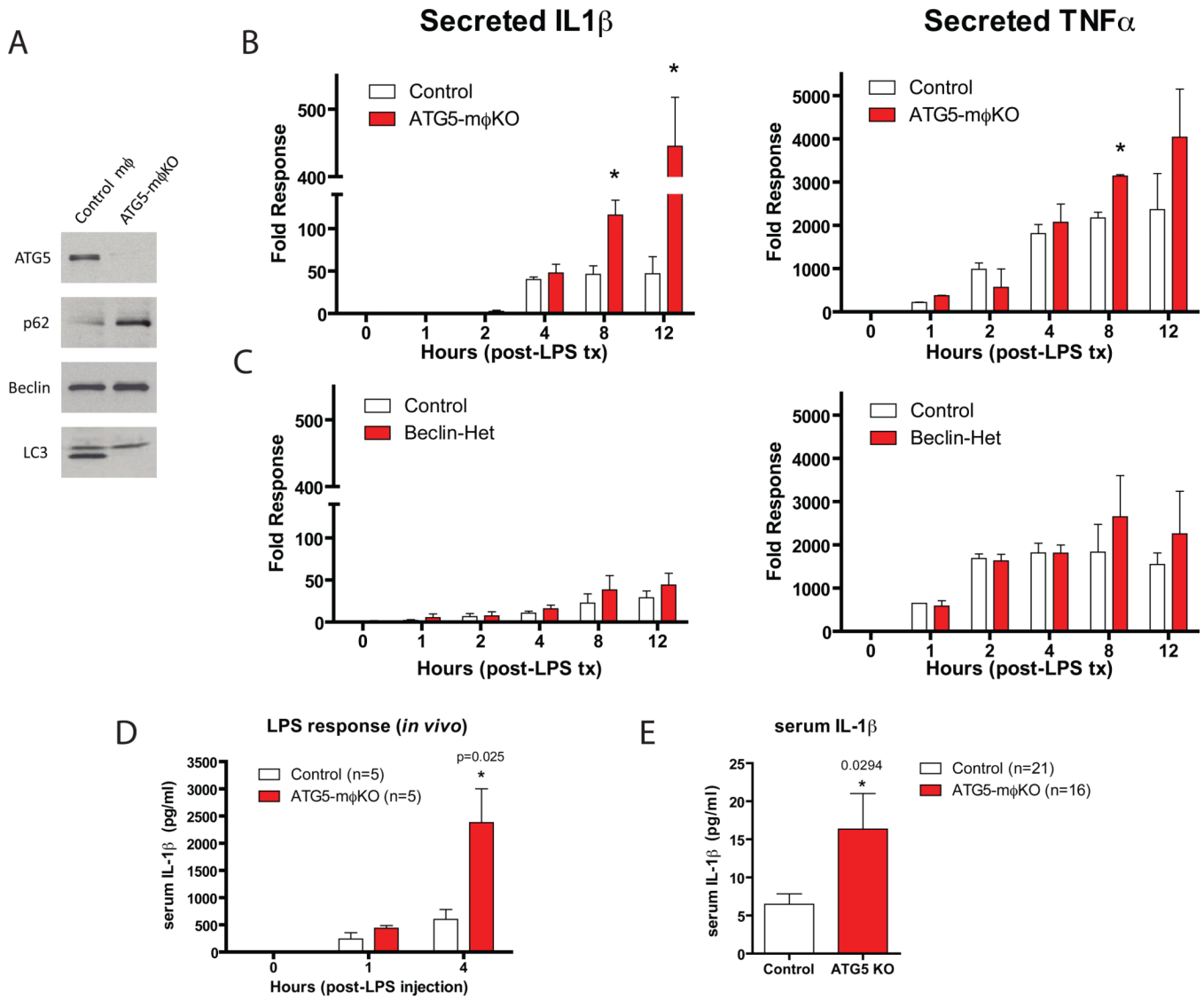

Figure 3. Comparison of the Pro-inflammatory Response of Beclin-Het and ATG5-mϕKO Macrophages

Experiments in (A–C) utilized cultured thioglycollate-elicited peritoneal macrophages.

(A) Western blot analysis of ATG5, p62, Beclin-1, and LC3 expression in macrophages derived from control vs. ATG5-mϕKO mice.

(B) Macrophages from control vs. ATG5-mϕKO mice treated with LPS (100 ng/ml) for the indicated times (in hours). Cell culture supernatants were assayed for IL-1β (left panel) and TNF-α (right panel) concentration by ELISA.

(C) Experiments identical to (B) except using macrophages from control vs. Beclin-Het mice. Experiments were performed in duplicate.

(D) Cohorts of control and ATG5-mϕKO mice were injected intraperitoneally with LPS (3.5 mg/g) and serum IL-1β at the indicated time points (in hours) was measured by ELISA.

(E) Cohorts of control and ATG5-mϕKO each on the ApoE-null background were fed a Western diet for 2 months. Serum IL-1β concentration was analyzed by ELISA.

Data are presented as mean ± SEM. *P<0.05 (exact P value shown).

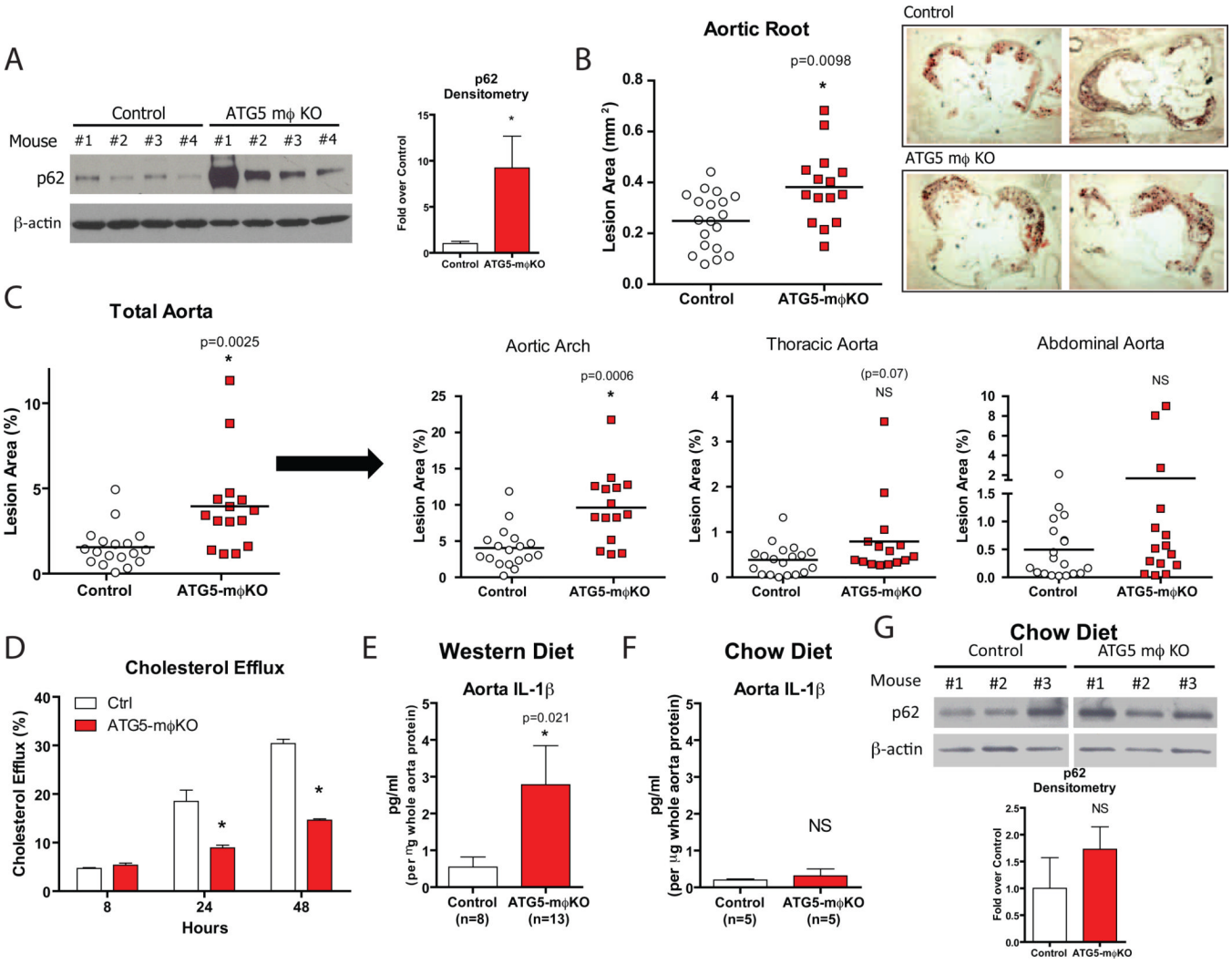

Figure 4. Quantification of Atherosclerosis in the ATG5-mϕKO Autophagy-Deficient Model

(A) Western blot analysis of p62 and β-actin in whole aorta lysates from control (n=4) and ATG5-mϕKO (n=4) mice (ApoE-null background) fed a Western diet for 2 months. Densitometric quantification is shown at right. *P<0.05.

(B, C) Cohorts of control and ATG5-mϕKO mice (ApoE-null background, # of mice shown) were fed a Western diet for 2 months and atherosclerotic area involvement was determined by computer image analyses. (B) Oil Red O-stained sections of aortic roots (representative aortic root sections are shown on the right). (C) *En face* results for the total aorta and its regions (aortic arch, thoracic aorta, and abdominal aorta). Horizontal lines within the data sets represent means. *P<0.05 (exact P value shown), NS = not significant.

(D) Cholesterol efflux to apoAI in AcLDL-loaded control and ATG5-mϕKO peritoneal macrophages over a 8, 24, and 48 hour time-course. *P<0.05.

(E, F) Cohorts of control and ATG5-mϕKO mice each on the ApoE-null background were fed a Western diet (E) or a chow diet (F) for 2 months. IL-1β concentration from whole aorta lysates was analyzed by ELISA.

(G) Western blot analysis of p62 and β-actin in whole aorta lysates from representative chow diet-fed mice with the densitometric quantification shown below. *P<0.05 (exact P value shown), NS = not significant.

For all panels, data are presented as mean ± SEM.

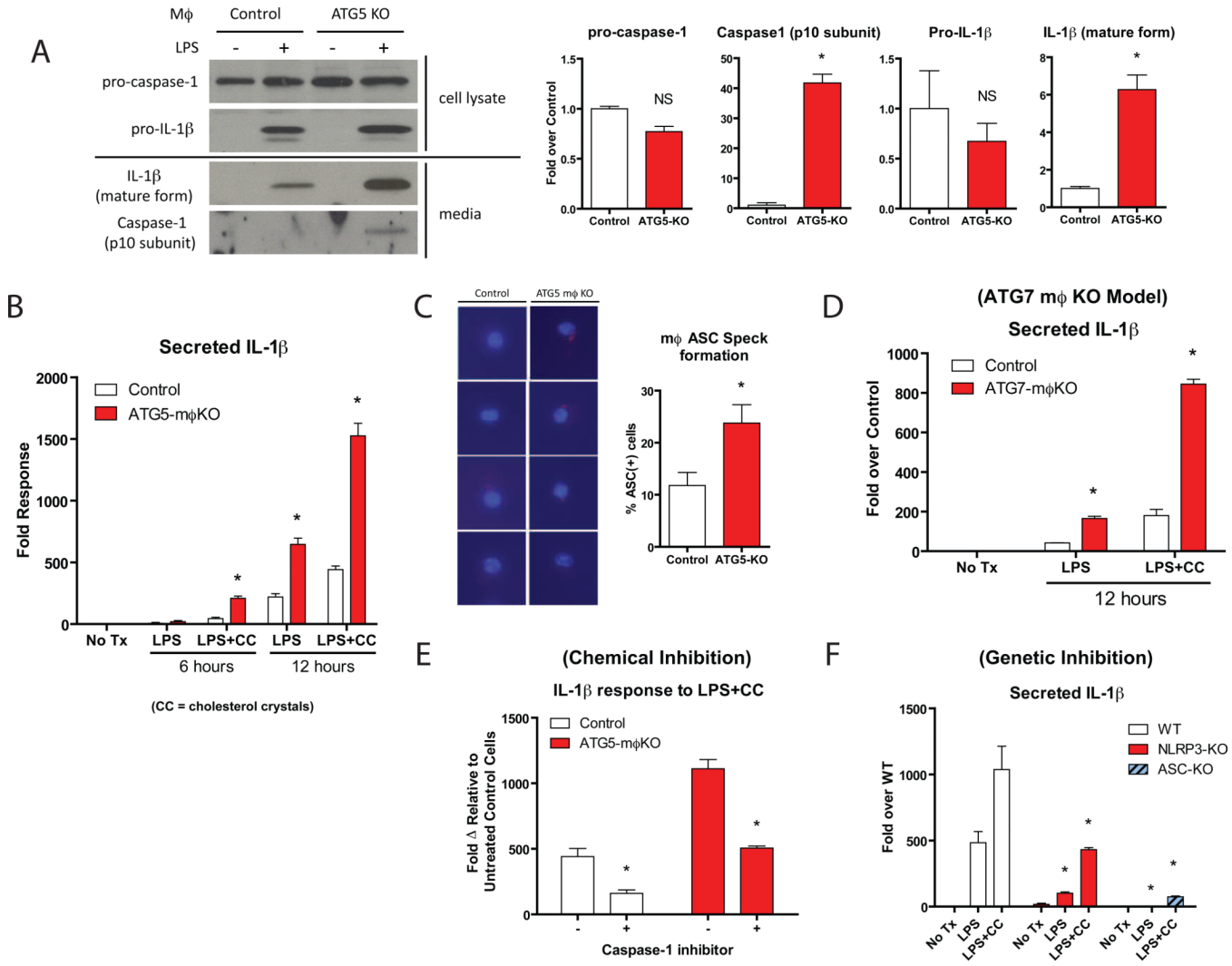

Figure 5. Inflammasomes are Synergistically Activated by Cholesterol Crystals and are Characteristic of Autophagy-Deficient Macrophages

Experiments in (A–E) utilized cultured thioglycollate-elicited peritoneal macrophages from control vs. ATG5-mϕKO mice (A–C,E) or ATG7-mϕKO mice (D).

(A) Macrophages were treated with or without LPS (100 ng/ml) for 12 hours. Western blot analysis of pro-caspase-1 and pro-IL-1β from macrophage cell lysates (top panels) and the cleaved/activated forms of caspase-1 (p10 subunit) and IL-1β secreted into the cell culture medium (lower panels) are shown. Densitometric quantification of Western blots from two separate experiments is shown at right. *P<0.05, NS = not significant.

(B) Macrophages were treated with or without LPS (100 ng/ml) or LPS (100 ng/ml) +cholesterol-crystals (CC, 500 μg/ml) for the indicated times (in hours). Cell culture supernatants were assayed for IL-1β concentration by ELISA. Experiments were performed in duplicate. *P<0.05.

(C) Macrophages were treated with LPS+cholesterol-crystals for 12 hours and ASC aggregation speck formation was determined by immunofluorescence microscopy. Four representative merged stains of ASC (red “specks”) and DAPI nuclear stains (blue) are shown for control and ATG5-mϕKO macrophages. The percentage of cells staining positive for ASC is quantified on the right.

(D) Control and ATG7-mϕKO macrophages were treated with LPS and LPS+cholesterol crystals for 12 hours. Cell culture supernatants were assayed for IL-1β concentration by ELISA. Experiments were performed in duplicate. *P<0.05.
(E) Macrophages were treated with LPS+cholesterol crystals for 12 hours in the presence or absence of a caspase-1 inhibitor and cell culture supernatants were assayed for IL-1β concentration by ELISA. Experiments were performed in duplicate. *P<0.05.
(F) Bone marrow-derived macrophages from wild-type, NLRP3-null, or ASC-null mice were treated with LPS or LPS+cholesterol crystals for 12 hours and cell culture supernatants were assayed for IL-1β concentration by ELISA. Experiments were performed in duplicate. *P<0.05.
For all panels, data are presented as mean ± SEM.

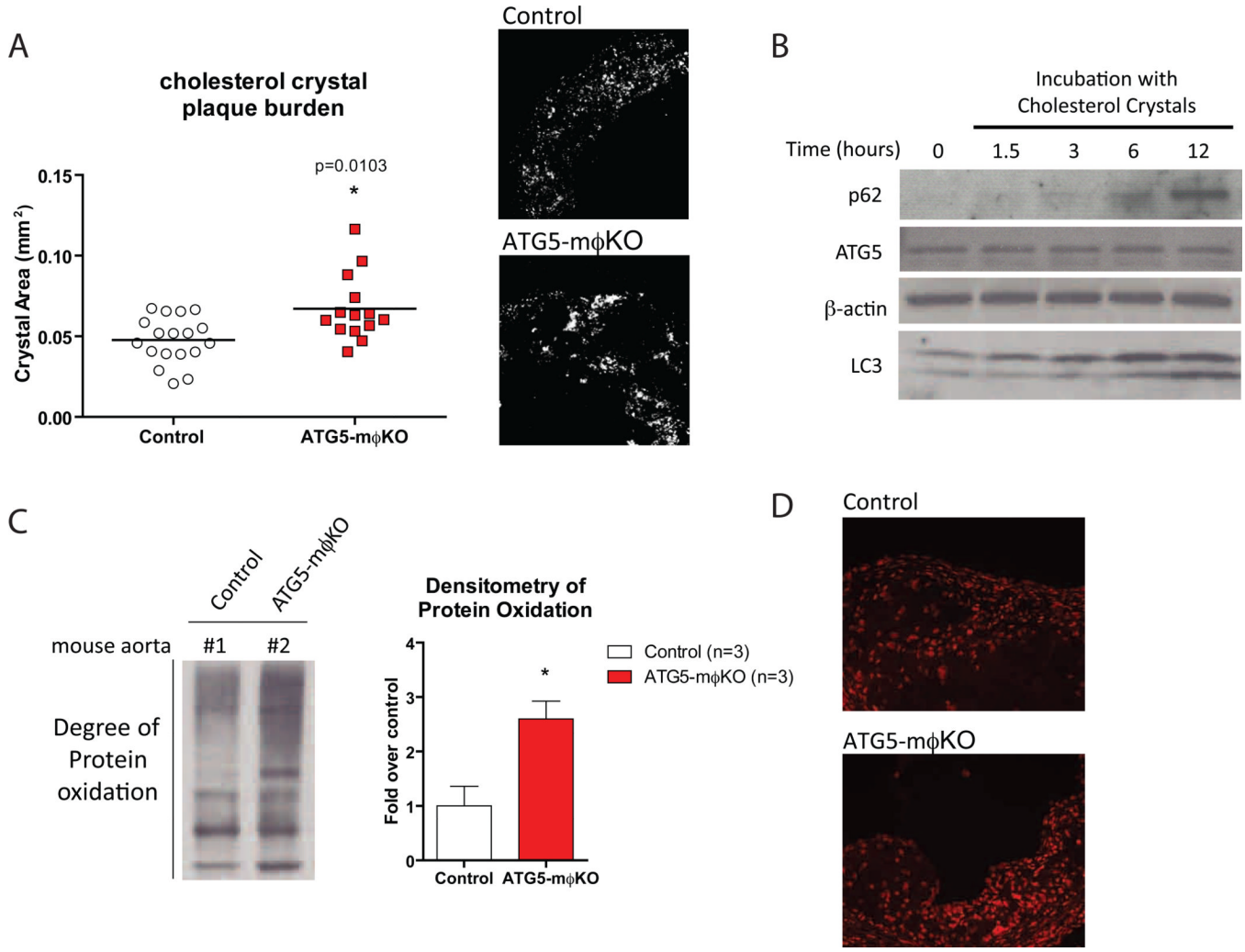

Figure 6. Increased Cholesterol Crystal Burden and Reactive Oxygen Species in ATG5-mϕKO Plaques are Potential Mediators of Atherosclerotic Progression

(A) Confocal reflectance microscopy of formaldehyde-fixed frozen-section aortic roots from cohorts of Western diet-fed control and ATG5-mϕKO (ApoE-null background) mice. Plaque cholesterol crystal burden was quantified by computer image analysis. Horizontal lines within the data sets represent means. *P<0.05 (exact P value shown). Reflectance images for a representative area of the aortic root are shown on the right.

(B) Western blot analysis of p62, ATG5, β-actin, and LC3 expression in wild type thioglycollate-elicited peritoneal macrophages incubated with cholesterol crystals (500 μg/ml) for the indicated times (in hours).

(C) Determination of protein oxidation in Western diet-fed control and ATG5-mϕKO (ApoE-null background) whole aortic lysates using the OxyBlot™ immunoblot detection assay. Densitometric analysis of control (n=3) and ATG5-mϕKO (n=3) mice is also shown. *P<0.05.

(D) The use of another oxidative stress marker, Dihydroethidium (DHE)-staining, in representative aortic root sections of mice. Higher intensity nuclear fluorescence is indicative of increased superoxide levels.

For all panels, graphical data are presented as mean ± SEM.

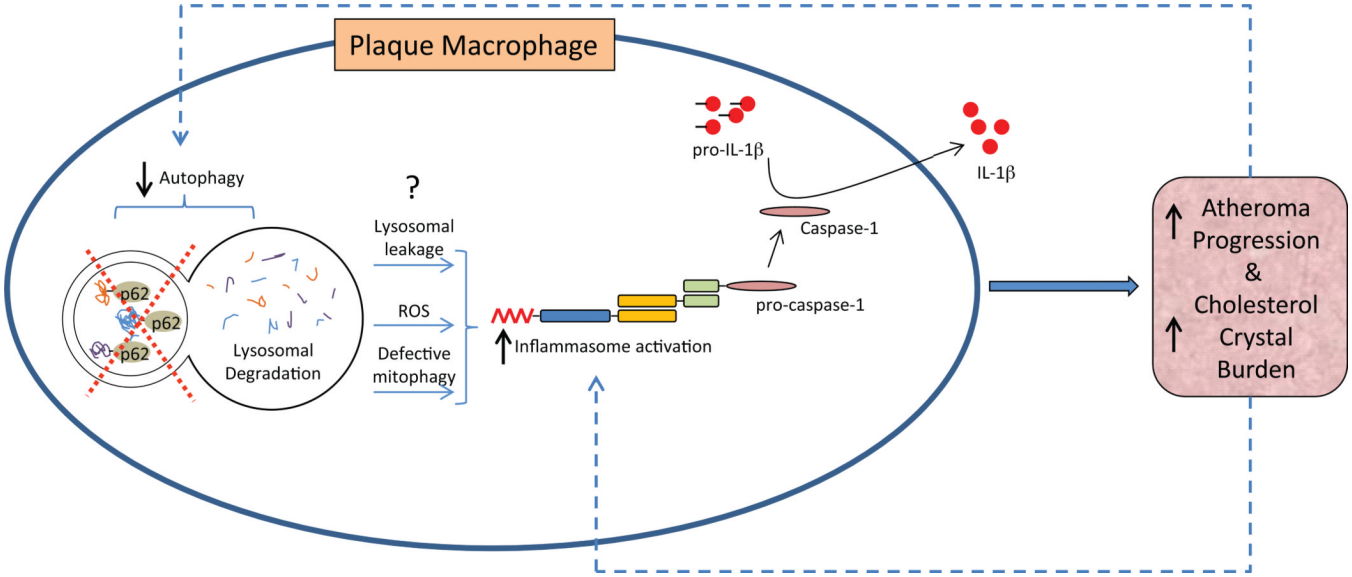

Figure 7. Schematic Depiction of the Links between Autophagy, Inflammasomes, and Atherosclerotic Progression